



Electromagnetic ferrofluid-based energy harvester

A. Bibo, R. Masana, A. King, G. Li, M.F. Daqaq*

Nonlinear Vibrations and Energy Harvesting Laboratory (NOVEHL), Department of Mechanical Engineering, Clemson University, Clemson, SC 29634, USA

ARTICLE INFO

Article history:

Received 14 January 2012
 Received in revised form 29 April 2012
 Accepted 15 May 2012
 Available online 17 May 2012
 Communicated by P.R. Holland

Keywords:

Ferrofluid
 Energy harvesting
 Electromagnetic
 Sloshing

ABSTRACT

This Letter investigates the use of ferrofluids for vibratory energy harvesting. In particular, an electromagnetic micro-power generator which utilizes the sloshing of a ferrofluid column in a seismically-excited tank is proposed to transform mechanical motions directly into electricity. Unlike traditional electromagnetic generators that implement a solid magnet, ferrofluids can easily conform to different shapes and respond to very small acceleration levels offering an untapped opportunity to design scalable energy harvesters. The feasibility of the proposed concept is demonstrated and its efficacy is discussed through several experimental studies.

© 2012 Elsevier B.V. All rights reserved.

1. Introduction

During the last decade, vibratory energy harvesting has become a focal area of research offering unprecedented opportunities to provide a continuous power supply for low-power consumption electronics where battery replacement is costly, difficult, or hazardous [1–5]. The underlying concept lies in the extraction of mechanical energy from the environment by exploiting the ability of active materials and various electromechanical coupling mechanisms to generate an electric potential in response to mechanical stimuli. Among the various energy harvesting mechanisms, electromagnetic transduction has been investigated extensively in the open literature [6–10]. Different configurations have been proposed, with the basic principle remaining the same; external vibrations set a *solid* magnet in motion relative to a stationary coil. As per Faraday's law, the change in magnetic flux produces a current in the coil which can then be channeled into an electric load.

In this Letter, the use of ferrofluids as the magnetic material in electromagnetic energy harvesters is investigated. Ferrofluids are colloidal liquids made of nano-scale permanent magnetic dipoles. As shown in Fig. 1, in the absence of an external magnetic field, the magnetic dipoles are randomly oriented in a carrier fluid and the magnetization of the fluid is zero. When an external magnetic field is applied, the dipoles rotate and produce a net magnetic moment such that the average direction of the fluid magnetization is parallel to the external field. In such a scenario, when a container carrying the magnetized fluid is subjected to seismic excitations

with a frequency that matches one of the infinite modal frequencies of the fluid column (resonance conditions), large amplitude surface waves, both horizontal and rotational, are excited. The motion of the sloshing liquid changes the orientational order of the magnetic dipoles and creates a time-varying magnetic flux. This flux induces an electromotive force in a coil wound around the container generating an electric current.

Unlike solid-state magnets, ferrofluids can conform to any shape and can be easily injected into hard-to-access locations opening avenues for fabricating scalable electromagnetic energy harvesters that can be operated in unique environments. In addition to this desired characteristic, it will be shown in this Letter that the modal frequencies of a ferrofluid based harvester can be tuned and reduced to very low values allowing for effective energy harvesting from the most common low-frequency excitations. Unlike solid-state magnets, the harvester can also respond at infinite closely-spaced modal frequencies which can improve its performance under random and non-stationary excitations.

2. Modal frequencies of the fluid column

To investigate the feasibility of the proposed concept, the experimental setup shown in Fig. 2 is constructed. A cylindrical container with a diameter of 32 mm and a height of 55 mm is mounted on an electrodynamic shaker which supplies seismic excitations of different magnitudes and frequencies. The external magnetic field is generated using two axially-magnetized permanent magnets. The ferrofluid used is a light hydrocarbon-based 15% by volume concentration of fine magnetite particles, Fe_3O_4 . Its density and magnetic susceptibility are given as $\rho = 1.21 \text{ g/cm}^3$, and $\chi = 1.552$, respectively. A cylindrical coil of 1000 winds is used.

* Corresponding author. Tel.: +1 864 656 7471; fax: +1 864 656 4435.
 E-mail address: mdaqaq@clemson.edu (M.F. Daqaq).

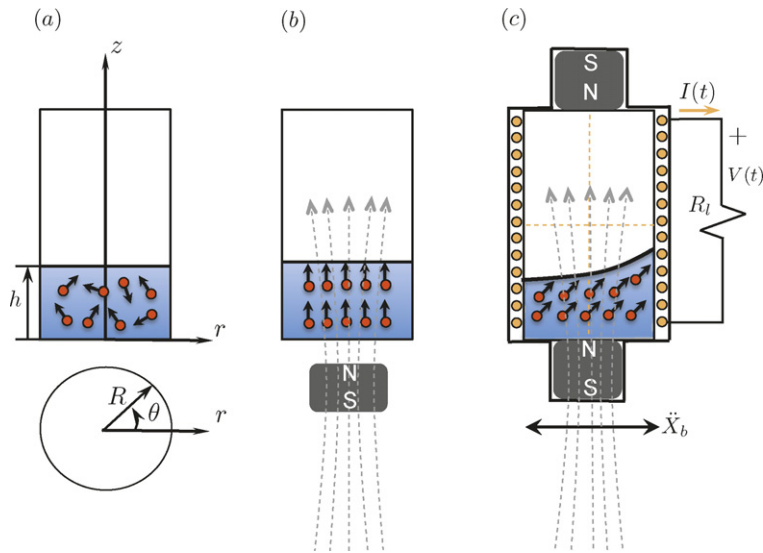


Fig. 1. Schematic diagram of the ferrofluid-based energy harvester.

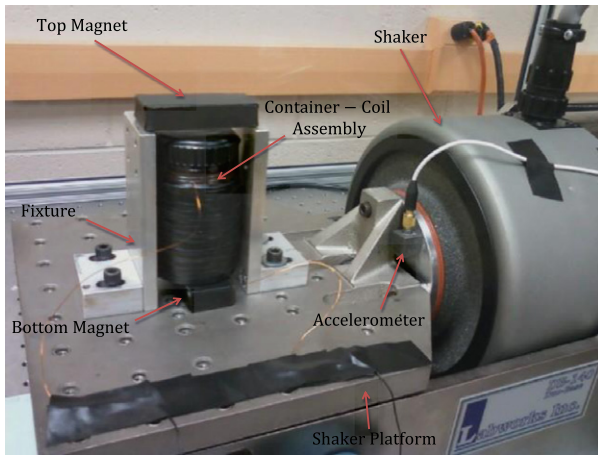


Fig. 2. Experimental setup.

The coil inductance, L , and resistance, R_c were measured at 20 mH and 37.5Ω , respectively.

Resonant motions are critical to produce large amplitude surface waves, which are, in turn, essential to produce a measurable change in the magnetic flux across the harvesting coil. These resonances occur near the undamped modal frequencies of the fluid column, which are given by [11,12] (assuming small surface waves while neglecting the influence of surface tension):

$$f_{mn} = \frac{1}{2\pi} \sqrt{\frac{g^* k_{mn}}{R} \tanh\left(\frac{k_{mn} h}{R}\right)}, \quad (1)$$

where the subscripts m and n indicate different oscillation modes. When m is even, the waves are symmetric (rotational) about the origin and the net change in magnetic flux is very small. On the other hand, when m is odd, the waves are asymmetric (horizontal) with a nodal diameter through the origin perpendicular to the direction of excitation. Here, h is the liquid height; R is the radius of the container, k_{mn} are the roots of $dJ_m(k_{mn}r/R)/dr|_{r=R} = 0$, where $J_m(\cdot)$ are the Bessel functions of the first kind and order m ; and g^* is the effective acceleration due to the gravitational and magnetic fields and is given by

$$g^* = g - \frac{\chi}{\rho\mu_0} \frac{dB(z)}{dz} B(z) \Big|_{z=h}, \quad (2)$$

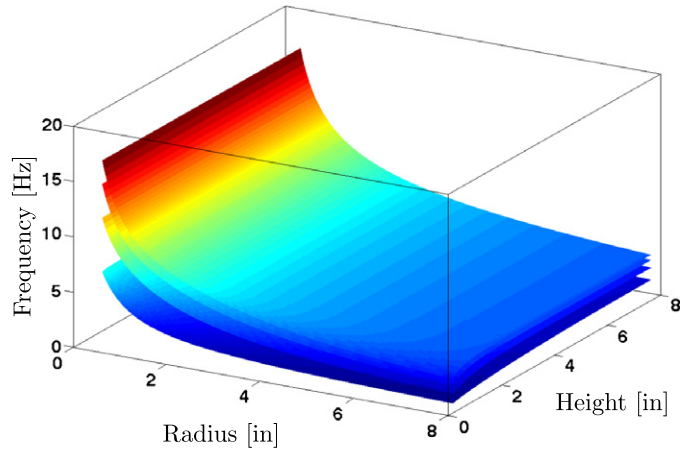


Fig. 3. Variation of the first four modal frequencies associated with the sloshing dynamics of the fluid column. Results are obtained in the absence of an external magnetic field.

where g is the gravitational acceleration and μ_0 is the magnetic permeability of vacuum. The term $B(z)$ represents the magnetic induction along the normal center line resulting from the lower and upper permanent magnets.

Variation of the first four modal frequencies of the response with the height of the fluid column and radius of the container is shown in Fig. 3. For a given height, the modal frequencies can be decreased by increasing the radius of the container and vice versa. This offers unique capabilities for tuning the harvester's modal frequency to low-frequency excitations which are very common in nature. Furthermore, due to the presence of infinite number of closely-spaced modal frequencies, a ferrofluid-based harvester can respond to random wide-band excitations.

Fig. 4 depicts variation of the two first asymmetric modal frequencies, f_{11} and f_{12} with the ferrofluid height as obtained theoretically and experimentally for the setup shown in Fig. 2. The magnetic induction was obtained experimentally using a Gauss meter and is depicted in Fig. 4(a). Both frequencies decrease with the liquid height, h , because the effective gravitational field g^* decreases as the height of the fluid column increases for a given magnetic field distribution. Both of the theory and experiment reveal similar trends with the experimental values slightly underestimating the theoretical ones due to neglecting the effect of viscous damping in the theoretical model.

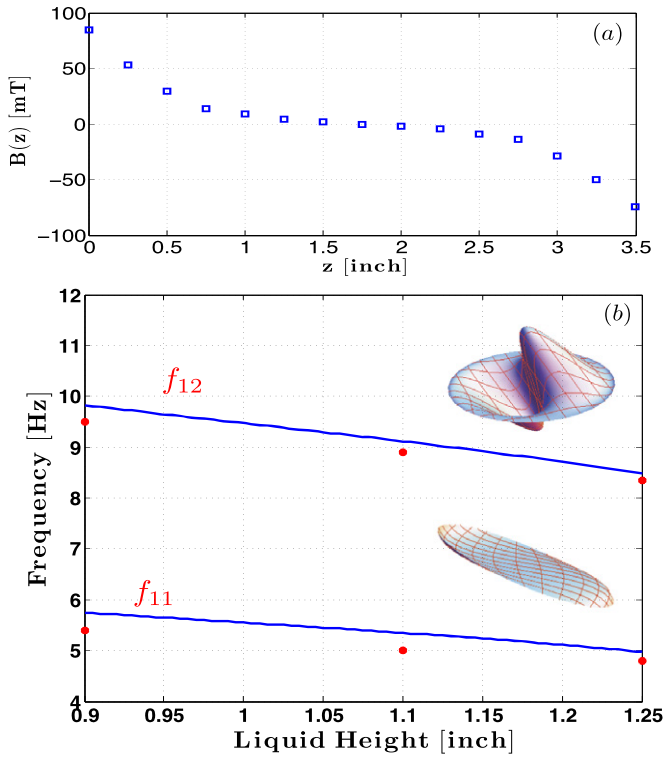


Fig. 4. (a) Magnetic field induction along the normal center line of the container. (b) Variation of the first two asymmetric modal frequencies with the fluid height.

3. Output voltage and power

After identifying the frequency spectrum within which the first two asymmetric modal frequencies are located, the harvester is subjected to harmonic base excitations with a slowly-varying frequency spanning the identified range. The steady-state open-circuit voltage of the harvester is measured. Fig. 5(a) investigates the influence of the fluid height on the output voltage for a given magnetic field strength and input acceleration level. For each height, two response peaks clearly appear in the voltage–frequency spectra, one near the first asymmetric modal frequency, f_{11} , and the other near the second asymmetric modal frequency, f_{12} .

Since the fluid experiences its largest deformations near the surface, the number and orientation of the dipoles closest to the surface are the most critical for the energy harvesting process. The number of dipoles is mainly characterized by the cross-sectional area of the container and the percentage of magnetic dipoles per unit volume of the fluid. As such, it is clearly evident in Fig. 5(a), that the height of the fluid column has a very little influence on the amplitude of output voltage.

Fig. 5(b) investigates the influence of the magnetic field strength on the output voltage of the harvester. The field is altered by changing the distance between the lower magnet and the bottom surface of the container as shown in Fig. 6. Results demonstrate that the magnetic field simultaneously influences the peak frequency and peak voltage of the harvester. As for the peak frequency; when the magnetic field induction near the surface of the fluid decreases from positive to negative values ($B(h) = 1.8 \text{ mT}$, -1.23 mT , -2.1 mT), the peak frequency decreases because the effective acceleration g^* decreases ($g^* = 11 \text{ m/s}^2$, 8.8 m/s^2 , 8.5 m/s^2). Therefore, by changing the external magnetic field, the frequency of the fluid column can be effectively shifted towards lower and higher frequencies, offering unique tunability characteristics.

As for the effect of the field strength and its spatial distribution on the peak voltage, it can be understood by examining Fig. 5(b)

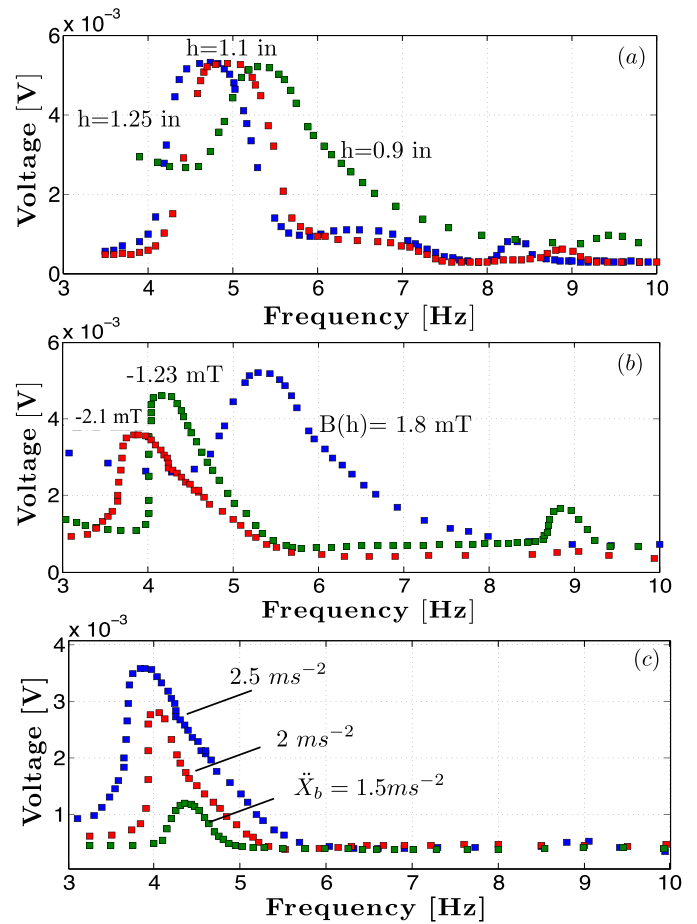


Fig. 5. Voltage–frequency response curves for (a) different liquid heights, $\ddot{X}_b = 2.5 \text{ m/s}^2$, (b) different magnetic field strength, $h = 0.9 \text{ in}$, $\ddot{X}_b = 2.5 \text{ m/s}^2$, and (c) different acceleration levels, and $h = 0.9 \text{ in}$.

in conjunction with Fig. 6. While, in general, the output voltage is mainly characterized by the number and orientation of the magnetic dipoles near the surface; the strength of magnetic field also plays a critical role by characterizing the coupling strength between the dipoles and the field. If the coupling is too weak, the dipoles become randomly oriented and the net flux is very small. If the coupling is too strong, very large base accelerations become necessary to rotate the magnetic dipoles with respect to the field. As shown in Fig. 6(a), when the magnetic field is positive throughout the fluid column, the magnetic dipoles are all oriented in the same direction with the external field. External excitations rotate the dipoles relative to the magnetic field in the same direction as the propagating wave. The change of magnetic flux due to the rotation of each dipole adds up and the output voltage of the harvester increases.

When the magnetic field changes direction within the fluid, as shown in Fig. 6(b), the dipoles that experience the weakest magnetic field orient themselves in a random fashion producing very small net flux as they move which reduces the output voltage. In the case when the lower magnet is placed at even a larger distance from the bottom surface of the container as shown in Fig. 6(c), the magnetic field at the surface becomes very larger in absolute value (2.1 mT versus 1.23 mT). As a result, the magnetic dipoles closest to the surface experience very strong coupling to the external field necessitating even larger base accelerations to produce sufficient relative rotations with respect to the field. This has the adverse influence of reducing the output voltage even further

Fig. 5(c) depicts the influence of the acceleration level on the output voltage. Clearly, the response exhibits a softening nonlinear

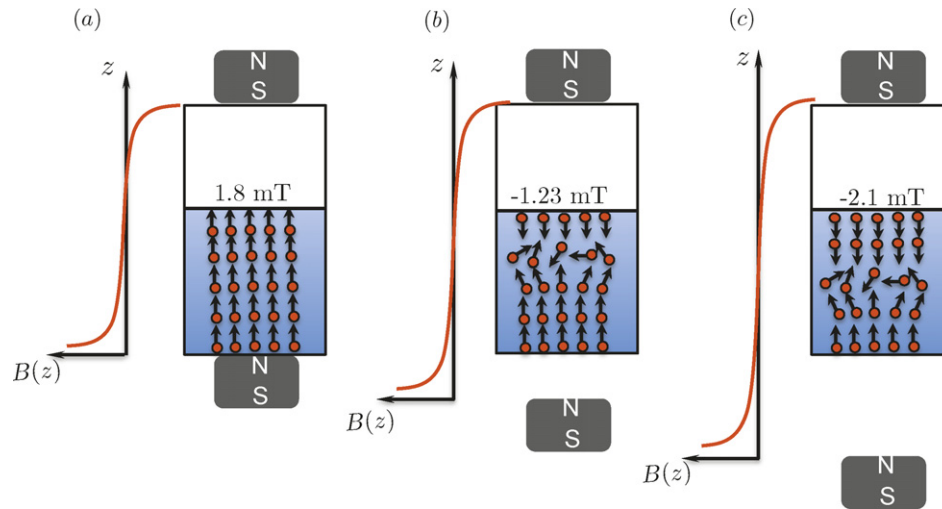


Fig. 6. A schematic showing the distribution of the magnetic dipoles in the ferrofluid for different magnetic field intensity.

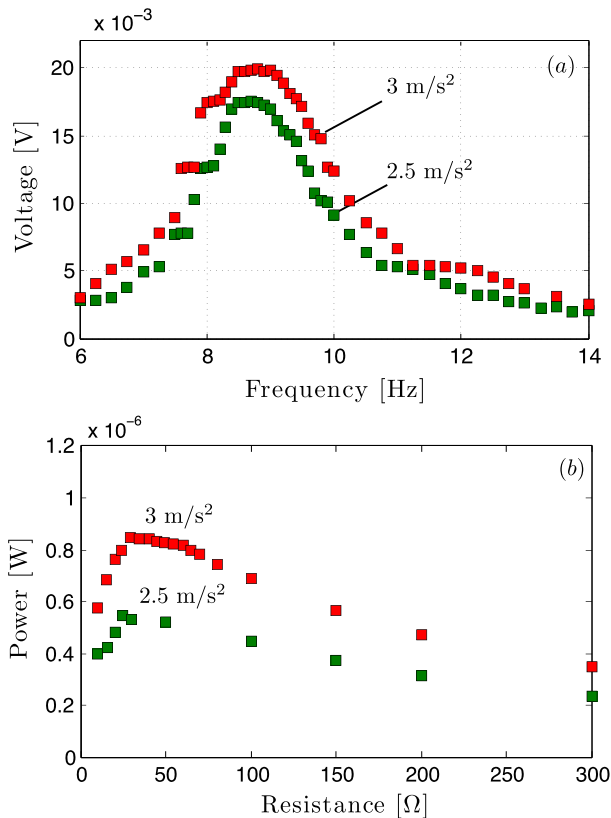


Fig. 7. (a) Frequency response and (b) power resistance curves for the harvester operating in the horizontal configuration. The power curves are obtained at a frequency of 9 Hz.

behavior with large amplitude responses shifting towards smaller frequencies as the magnitude of input acceleration increases.

To confirm that the number of dipoles near the surface plays the most critical role in determining the output voltage of the harvester, the surface area of the fluid was increased by tilting the container sideways by 90° such that the container lays horizontally rather than in the upright position. The open-circuit voltage and output power across different resistive loads are measured for different acceleration levels as shown in Fig. 7. It is evident that

the output voltage of the harvester increases significantly as the surface area increases. For instance, the peak output voltage at $\ddot{X}_b = 2.5 \text{ m/s}^2$ increases from 3.5 mV in the upright position to about 18 mV when the container is tilted sideways. The associated power curves demonstrate that the generator can produce around $1 \mu\text{W}$ of power at an optimal resistance of around 35Ω .

4. Conclusion

The results presented in the Letter demonstrate the feasibility of the proposed ferrofluid based energy harvester concept. While the attained power levels are still small as compared to the traditional electromagnetic energy harvesters, it is our belief that a ferrofluid based harvester has some unique advantages and can prove very beneficial in some targeted applications where the utilization of a moving solid magnet is not possible. Additionally, with the development of proper theoretical models to capture the response behavior of the harvester, the design parameters can be further optimized to improve the harvester's performance.

Acknowledgements

This material is based upon work supported by the National Science Foundation under Grant No. 1000667. Any opinions, findings, and conclusions or recommendations expressed in this material are those of the author and do not necessarily reflect the views of the National Science Foundation.

References

- [1] S. Roundy, P.K. Wright, J. Rabaey, *Computer Communications* 26 (2003) 1131.
- [2] S. Priya, *Applied Physics Letters* 87 (2005) 184101.
- [3] N. Elvin, N. Lajnef, A. Elvin, *Smart Materials and Structures* 15 (2006) 977.
- [4] D. Jia, J. Liu, Y. Zhou, *Physics Letters A* 373 (2009) 1305.
- [5] M. Lallart, S. Pruvost, D. Guyomar, *Physics Letters A* 377 (2011) 3921.
- [6] C. Shearwood, R. Yates, *Electronics Letters* 33 (1997) 1883.
- [7] R. Amirtharajah, A. Chandrakasan, *IEEE Journal of Solid-State Circuits* 33 (1998) 687.
- [8] C. Williams, C. Shearwood, M. Harradine, P. Mellor, T. Birch, *IEE Proceedings: Circuits, Devices and Systems* 148 (1998) 337.
- [9] C. Serre, A. Perez-Rodriguez, N. Fondevilla, E. Martincic, S. Martinez, J. Morante, J. Montserrat, J. Esteve, *Microsystem Technologies* 14 (2008) 653.
- [10] B. Mann, N. Sims, *Journal of Sound and Vibrations* 319 (2008) 515.
- [11] F. Matsuura, Y. Matsubara, T. Sawada, T. Tanahashi, *Advanced Computational and Design Techniques in Applied Electronic Systems* (1995) 517.
- [12] J. Neuringer, R. Rosensweig, *Physics of Fluids* 7 (1964) 1927.